

# Final state interactions for $B \rightarrow VV$ charmless decays

**Massimo Ladisa, Vincenzo Laporta, Giuseppe Nardulli**

*Dipartimento di Fisica dell'Università di Bari, Italy  
Istituto Nazionale di Fisica Nucleare, Sezione di Bari, Italy*

**Pietro Santorelli**

*Dipartimento di Scienze Fisiche, Università di Napoli "Federico II", Italy  
Istituto Nazionale di Fisica Nucleare, Sezione di Napoli, Italy*

We estimate final state interactions in the  $B$ -meson decays into two light vector mesons by the Regge model. We consider Pomeron exchange and charmed Regge trajectories that can relate intermediate charmed particles to the final state. The Regge poles have various helicity-flip residues, which allows a change from the longitudinal to transverse polarization. In this way a significant reduction of the longitudinal polarization fraction can be produced. In the factorization approximation we find agreement with recent data from the BaBar and Belle collaborations in the  $B \rightarrow K^* \phi$  decay channel, as a result of an appropriate choice of semileptonic form factors and Regge exchanges. On the other hand, data for the  $K^* \rho$  decay channels appear more elusive. The soft effects discussed in the present paper are based on a model of Regge trajectories that is shown to reproduce correctly in the non-charmed case the Regge phenomenology of light mesons.

PACS numbers: 13.25.Hw

## I. INTRODUCTION

Recent data from the Babar and Belle collaborations [1–4] on the  $B$  decays into two light vector mesons  $B \rightarrow VV$  have produced considerable theoretical interest, see e.g. the recent papers [5–8]. Data for the Branching Ratios (BR) and the polarization fractions for a few decay channels are reported in Table I.

Decay mode	BR	$\Gamma_L/\Gamma$	$\Gamma_\perp/\Gamma$	Ref.
$B^+ \rightarrow \rho^0 K^{*+}$	$(10.6^{+3.0}_{-2.6} \pm 2.4) \times 10^{-6}$	$0.96^{+0.04}_{-0.15} \pm 0.04$		[1],[2]
$B^+ \rightarrow \phi K^{*+}$	$(9.5 \pm 1.7) \times 10^{-6}$	$0.46 \pm 0.12 \pm 0.03$		[1],[3]
$B^0 \rightarrow \phi K^{*0}$	$(10.7 \pm 1.2) \times 10^{-6}$	$0.58 \pm 0.06$	$0.41 \pm 0.10 \pm 0.02$	[1],[3]
$B^+ \rightarrow \rho^0 \rho^+$	$(26.2 \pm 6.2) \times 10^{-6}$	$0.96 \pm 0.07$		[1],[2],[4]
$B^0 \rightarrow \rho^+ \rho^-$	$(25^{+7+5}_{-6-6}) \times 10^{-6}$	$0.98^{+0.02}_{-0.08} \pm 0.03$		[1],[2]

TABLE I: Survey of experimental results for  $B$  decays into two light vector mesons. Data of Refs.[1] and [2] are from the BaBar collaboration. Data from Refs. [3] and [4] are from the Belle Collaboration. There is also an upper bound  $\mathcal{B}(B^0 \rightarrow \rho^0 \rho^0) \leq 2.1 \times 10^{-6}$  from BaBar [1].

In these decay modes the two vector mesons have the same helicity; therefore three different polarization states are possible, one longitudinal ( $L$ ) and two transverse, corresponding to helicities  $\lambda = 0$  and  $\lambda = \pm 1$ . We define the corresponding amplitudes as  $A_{0,\pm}$ . It is easy to show [5] that in the large  $m_b$  limit longitudinal polarization must be enhanced by a factor of  $m_b$  in the amplitude. This can be seen at the quark level, the reason being that transverse polarizations are generated by helicity flip and this implies an extra factor  $m_V/m_b$ . Alternatively, at the hadronic level, by making use of naive factorization, one traces back the enhancement of the longitudinal polarization to the presence of an extra factor  $m_B/m_V + \mathcal{O}((m_V/m_B)^2)$  in the longitudinal polarization vectors. The enhancement in the longitudinal amplitude is of one power of  $m_b$ . In fact the term with two powers is multiplied by the difference  $A_1 - A_2$  where  $A_1$  and  $A_2$  are the usual axial form factors [9] for the transition  $B \rightarrow V$  computed at  $q^2 = m_V^2$ . This difference vanishes in the high  $m_b$  limit, see e.g. [10].

Decay modes  $B^0 \rightarrow \rho^+ \rho^-$  and  $B^+ \rightarrow \rho^0 \rho^+, \rho^0 K^{*+}$  confirm this prediction as the final states are dominated by the longitudinal polarization. On the other hand, for the observed  $B \rightarrow \phi K^*$  transitions, the longitudinal amplitude width gives about 50% of the rate. This is a major puzzling feature because, as argued above, in the naive factorization, one expects also for the  $\phi K^*$  channels

$$\frac{\Gamma_L}{\Gamma} = \frac{|A_0|^2}{|A_0|^2 + |A_+|^2 + |A_-|^2} = 1 - \mathcal{O}\left(\frac{1}{m_b^2}\right). \quad (1)$$

Another surprising aspect concerns the transverse polarization defined by

$$\Gamma_{\perp} \propto |A_{\perp}|^2, \quad (2)$$

where  $A_{\perp,\parallel} = (A_+ \mp A_-)/\sqrt{2}$ . Moreover, one expects [5]

$$\frac{\Gamma_{\perp}}{\Gamma_{\parallel}} = 1 + \mathcal{O}\left(\frac{1}{m_b}\right). \quad (3)$$

This expectation is based on naive factorization and large energy relations [10]. The former assumption implies that in the large  $m_b$  limit  $A_-$  is proportional to  $(A_1 - V)/(A_1 + V) + \mathcal{O}(m_V/m_B)$  where  $A_1$  and  $V$  are the usual form factors [9] for the transition  $B \rightarrow K^*$  computed at  $q^2 = m_{\phi}^2$ . The latter implies that  $(A_1 - V)/(A_1 + V) = \mathcal{O}(1/m_b)$ , a prediction confirmed by different numerical computations based on lattice QCD or QCD sum rules. As a consequence  $A_-/A_+ = \mathcal{O}(1/m_b)$  and (3) should hold. A result from Belle is reported in Table I, which is at odds with (3); a smaller result from BaBar [11]

$$\frac{\Gamma_{\perp}}{\Gamma} = 0.27 \pm 0.07 \pm 0.02 \quad (4)$$

has been also presented, which might be compatible with (3).

All previous considerations do not take into account final state interactions (FSI) that, although power suppressed, might nevertheless produce sizeable effects. In [7] a parametrization of these effects is considered. It assumes a major role of the so-called charming penguin diagrams. They are Feynman diagrams with intermediate  $D\bar{D}$  states [12–16]. The suppression due to their non-factorizable status might be compensated by the Cabibbo-Kobayashi-Maskawa (CKM) enhancement. The computational scheme used in [7] and in previous computations for  $B$  decays into two light particles [14–16] is chiral perturbation theory for light and heavy mesons (for a review see [17]). Since momenta of the final particles are hard, the application of the method involves large extrapolations and the method is questionable (see e.g. [8]). A possible answer consists of introducing some correction. In [14–16] such correction was modelled by a form factor evaluated by a constituent quark model. In [7] a phenomenological parameter  $r$  is introduced to weight the charming penguin contribution. Both approaches result in a suppression of charming penguin contributions, but uncertainties are huge.

The reason for the suppression can be traced back to the Regge theory. In fact, given the rather large energy involved ( $\sqrt{s} = m_B$ ), the Regge approach should be a good approximation for the final state interactions and provide a computational scheme of the rescattering effects, be they elastic or inelastic. The former are described by Pomeron exchange [18], [19]. Among the latter, one may still assume dominance of the charming penguin amplitudes, due to the CKM enhancement, but they should be evaluated *via* a reggeized amplitude. In this context the suppression of the charming penguin arises because the Regge charmed trajectories have a negative intercept  $\alpha(0)$  and therefore a suppression factor  $(s/s_0)^{\alpha(0)}$  ( $s_0 \simeq 1 \text{ GeV}^2$ , a threshold). The advantage of the Regge approach is to evaluate the intermediate charmed states contributions not by Feynman diagrams, but by unitarity diagrams and the Watson's theorem [20]. In this way the remarks connected to the extrapolation of chiral theory to hard momenta are by-passed.

The aim of this paper is to give an evaluation of the final state interactions for  $B \rightarrow VV$  using the Regge model. Clearly also the numerical values of the bare (no FSI) amplitudes are important. We compute them in the factorization approximation and therefore we need a set of semileptonic form factors as an input. We use a determination based on Light Cone QCD sum rules [21] that encompasses both the  $B \rightarrow K^*$  and the  $B \rightarrow \rho$  transitions. For  $B \rightarrow K^*$  we also use results obtained by QCD sum rules [22]. These results are summarized in section II. In section III we discuss rescattering effects as parametrized by the Regge model. We include in the parametrization the Pomeron and charmed Regge trajectories and we give estimates of the Regge residues. In section IV we present our numerical results and discuss them. The basic result we find is that, due to the presence of helicity-flip Regge residues, longitudinal polarization fractions are in general reduced, except for the  $B \rightarrow \rho\rho$  decay modes. Differences between the channels  $B \rightarrow K^*\phi$  and  $B \rightarrow K^*\rho$  might depend on the choice of the form factors, therefore we discuss differences induced by this choice as well. We argue that for the  $B \rightarrow K^*\phi$  decay mode an interplay between form factors and Regge parameters can produce theoretical results compatible with the data with no need to introduce new physics effects. For the  $B \rightarrow K^*\rho$  the results are more elusive and more work is needed especially for the determination of the semileptonic form factors. Finally in the Appendix we give an outline of the model used to compute the parameters of the charmed Regge trajectories.

## II. BARE AMPLITUDES

In this section we introduce bare amplitudes, i.e. matrix elements of the weak hamiltonian with no final state interaction effects. We consider two sets of weak bare amplitudes. The first set includes the bare amplitudes for the  $B$

decays into two light vector mesons. We consider the channels  $B \rightarrow \rho\rho$ ,  $B \rightarrow K^*\rho$ ,  $B \rightarrow K^*\phi$ . Since this calculation is straightforward we limit our presentation to the numerical results.

For the relevant Wilson coefficients we use  $a_1 = 1.05$ ,  $a_2 = 0.053$ , and  $(a_3, a_4, a_5, a_7, a_9, a_{10}) = (48, -439 - 77i, -45, +0.5 - 1.3i, -94 - 1.3i, -14 - 0.4i) \times 10^{-4}$  [23]. We use two different choices of form factors for the weak transition  $B \rightarrow V$ . The first choice is based on Light Cone QCD sum rules [21]. The corresponding results for the bare amplitudes for  $B \rightarrow K^*\rho$  and  $B \rightarrow \rho\rho$  are reported in Table II. We also consider the QCD Sum Rules results of Ref. [22]. Since in this paper only the  $b \rightarrow s$  transitions are considered, these results can be employed only for  $B \rightarrow K^*\phi$  decays. The numerical results obtained by the two sets of form factors for the  $B \rightarrow K^*\phi$  decay channel are reported in Table III.

Process	$\lambda$	$A_{b,\lambda}$	Process	$\lambda$	$A_{b,\lambda}$
$B^+ \rightarrow K^{*0}\rho^+$	0	$-0.62 + 3.14i$	$B^+ \rightarrow \rho^0\rho^+$	0	$+4.21 - 2.60i$
$B^+ \rightarrow K^{*0}\rho^+$	+	$+0.17 - 0.86i$	$B^+ \rightarrow \rho^0\rho^+$	+	$-1.01 + 0.62i$
$B^+ \rightarrow K^{*0}\rho^+$	-	$-0.02i$	$B^+ \rightarrow \rho^0\rho^+$	-	$-0.01 + 0.01i$
$B^+ \rightarrow K^{*+}\rho^0$	0	$+0.54 + 2.64i$	$B^0 \rightarrow \rho^+\rho^-$	0	$+5.60 - 3.93i$
$B^+ \rightarrow K^{*+}\rho^0$	+	$-0.15 - 0.70i$	$B^0 \rightarrow \rho^+\rho^-$	+	$-1.34 + 0.94i$
$B^+ \rightarrow K^{*+}\rho^0$	-	$-0.01i$	$B^0 \rightarrow \rho^+\rho^-$	-	$-0.02 + 0.01i$

TABLE II: Bare helicity amplitudes for  $B \rightarrow K^*\rho$  and  $B \rightarrow \rho\rho$  with form factors from Ref. [21]. Results in  $10^{-8}$  GeV.

Process	$\lambda$	$A_{b,\lambda}(\text{Ref. [21]})$	$A_{b,\lambda}(\text{Ref. [22]})$
$B \rightarrow K^*\phi$	0	$-0.83 + 3.85i$	$-0.48 + 2.24i$
$B \rightarrow K^*\phi$	+	$+0.27 - 1.25i$	$+0.28 - 1.30i$
$B \rightarrow K^*\phi$	-	$-0.03i$	$+0.01 - 0.06i$

TABLE III: Bare helicity amplitudes for  $B \rightarrow K^*\phi$  with two different choices of form factors [21] and [22]. Results in  $10^{-8}$  GeV.

We note the numerical relevance of  $A_0$  and the suppression of  $A_-$  in comparison with  $A_+$ . We also note numerical differences in Table III arising from the different choice of form factors.

The second set of amplitudes includes the bare decays of  $B^+$  into two charmed mesons,  $D_s^{(*)+} \bar{D}^{(*)0}$ . For the  $B \rightarrow \rho\rho$  decay channel we consider  $B$  decay into two charmed non strange mesons. The matrix elements of this second set are computed in the factorization approximation, using the Heavy Quark Effective Theory at leading order, with the following Isgur-Wise function  $\xi(\omega) = 4/(1 + \omega)^2$ . For the CKM matrix elements we use PDG data [24].

Numerical results for the bare helicity amplitudes  $A_{b,\lambda}$  for the channels  $B^+ \rightarrow D_s^{(*)+} \bar{D}^{(*)0}$  are reported in Table IV.

Process	$\lambda$	$A_{b,\lambda}^{(k)}$
$B^+ \rightarrow D_s^+ \bar{D}^0$	0	$+1.32i$
$B^+ \rightarrow D_s^+ \bar{D}^{*0}$	0	$-1.15i$
$B^+ \rightarrow D_s^{*+} \bar{D}^0$	0	$-1.15i$
$B^+ \rightarrow D_s^{*+} \bar{D}^{*0}$	0	$+1.32i$
$B^+ \rightarrow D_s^{*+} \bar{D}^{*0}$	+	$-1.02i$
$B^+ \rightarrow D_s^{*+} \bar{D}^{*0}$	-	$-0.42i$

TABLE IV: Bare helicity amplitudes for  $B$  decays into charmed mesons. The four channels  $B^+ \rightarrow D_s^+ \bar{D}^0$ ,  $B^+ \rightarrow D_s^{*+} \bar{D}^0$ ,  $B^+ \rightarrow D_s^{*+} \bar{D}^{*0}$ , and  $B^+ \rightarrow D_s^{*+} \bar{D}^{*0}$  are identified respectively by the index  $k = 1, 2, 3, 4$ . Units are  $10^{-6}$  GeV.

One can immediately notice the CKM enhancement (typically by a factor  $10^2$ ) of the amplitudes in Table IV in comparison with those of Table II. For  $B$  decay into two non-strange charmed mesons the enhancement is smaller.

### III. FINAL STATE INTERACTIONS AND REGGE BEHAVIOR

Corrections to the bare amplitudes due to final state interactions are taken into account by means of the Watson's theorem [20]:

$$A = \sqrt{S} A_b \quad (5)$$

where  $S$  is the  $S$ -matrix,  $A_b$  and  $A$  are the bare and the full amplitudes.

The two-body  $S$ -matrix elements are given by

$$S_{ij}^{(I)} = \delta_{ij} + 2i\sqrt{\rho_i \rho_j} T_{ij}^{(I)}(s) \quad , \quad (6)$$

where  $i, j$  run over all the channels involved in the final state interactions.

The  $J = 0$ , isospin  $I$  amplitude  $T_{ij}^{(I)}(s)$  is obtained by projecting the  $J = 0$  angular momentum out of the amplitude  $T_{ij}^{(I)}(s, t)$ :

$$T_{ij}^{(I)}(s) = \frac{1}{16\pi} \frac{s}{\sqrt{\ell_i \ell_j}} \int_{t_+}^{t_-} dt T_{ij}^{(I)}(s, t) \quad . \quad (7)$$

The momenta  $\rho_j, \ell_j$  are defined below. For the channel  $B \rightarrow K^* \phi$  we only have the  $I = 1/2$  transition amplitudes, for  $B \rightarrow K^* \rho$  both  $I = 1/2$  and  $I = 3/2$  are involved. For  $B \rightarrow \rho \rho$  we can have  $I = 0$  and  $I = 2$ .

As discussed in the Introduction, given the rather large value of  $s = m_B^2$ , a Regge approximation for the transition amplitude seems adequate. We will therefore include first of all the Pomeron term, which contributes to the elastic channels. For the inelastic channels we include only channels whose bare amplitudes are prominent. For  $B \rightarrow K^* \phi$  and  $B \rightarrow K^* \rho$  they should be the amplitudes for the transition  $B \rightarrow D^{(*)} D_s^{(*)}$  since these channels are Cabibbo enhanced, see table IV. For the  $I = 0$  amplitude of the decay  $B \rightarrow \rho^+ \rho^-$  there is no Cabibbo enhancement; most probably other trajectories should be considered, but we consider here again charmed trajectories mainly for the sake of comparison. The transition from a state with two charmed mesons to a state with two light particles can only occur *via* charmed Regge poles. Therefore in the present approximation we will include, besides the Pomeron, only the charmed Regge trajectories.

#### A. Pomeron contribution

To begin with we consider the Pomeron contribution. We write

$$S = \mathcal{P} \quad (8)$$

neglecting for the time being non leading Regge trajectories and inelastic terms. We have

$$\mathcal{P} = 1 + 2iT^{\mathcal{P}}(s), \quad T^{\mathcal{P}}(s) = \frac{1}{16\pi s} \int_{-s+4m_V^2}^0 T^{\mathcal{P}}(s, t) dt. \quad (9)$$

The following parametrization can be used [19], [25]:

$$T^{\mathcal{P}}(s, t) = -\beta^{\mathcal{P}} g(t) \left( \frac{s}{s_0} \right)^{\alpha_{\mathcal{P}}(t)} e^{-i\frac{\pi}{2}\alpha_{\mathcal{P}}(t)} \quad , \quad (10)$$

with  $s_0 = 1 \text{ GeV}^2$  and

$$\alpha_{\mathcal{P}}(t) = 1.08 + 0.25t \quad (t \text{ in } \text{GeV}^2) \quad , \quad (11)$$

as given by fits to hadron-hadron scattering total cross sections. The product  $\beta^{\mathcal{P}} \cdot g(t) = \beta^{\mathcal{P}}(t)$  represents the Pomeron residue; for the  $t$ -dependence we assume [19], [25]

$$g(t) = \frac{1}{(1 - t/m_\rho^2)^2} \simeq e^{2.8t} \quad . \quad (12)$$

To get  $\beta^{\mathcal{P}}$  we use factorization and the additive quark counting rule. For the  $B \rightarrow K^* \rho$  channel residue factorization gives

$$\beta_{K^* \rho}^{\mathcal{P}} = \beta_{\rho}^{\mathcal{P}} \beta_{K^*}^{\mathcal{P}} . \quad (13)$$

The two residues appearing in (13) can be computed by the additive quark counting rule. This gives [19]

$$\begin{aligned} \beta_{\rho}^{\mathcal{P}} &\sim \beta_{\pi}^{\mathcal{P}} = 2\beta_u^{\mathcal{P}} , \\ \beta_{K^*}^{\mathcal{P}} &\sim \beta_K^{\mathcal{P}} = \beta_u^{\mathcal{P}} + \beta_s^{\mathcal{P}} . \end{aligned} \quad (14)$$

The basis of the additive quark counting rule is given by pion-proton and proton-proton high energy scattering data. From these data [19],[26]:  $\beta_{\pi}^{\mathcal{P}} \sim 2/3\beta_p^{\mathcal{P}} \sim 5.1$ . From  $Kp$  high energy scattering data, one finds  $\beta_s^{\mathcal{P}} \sim 2/3\beta_u^{\mathcal{P}}$ . Therefore

$$\beta_{K^* \rho}^{\mathcal{P}} \approx 22 . \quad (15)$$

For the  $B \rightarrow K^* \phi$  channel we have, instead of Eq. (13),  $\beta_{K^* \phi}^{\mathcal{P}} = \beta_{\phi}^{\mathcal{P}} \beta_{K^*}^{\mathcal{P}}$ , and, numerically,  $\beta_{K^* \phi}^{\mathcal{P}} \approx 14$ . Finally for the  $B \rightarrow \rho \rho$  channel we get  $\beta_{\rho \rho}^{\mathcal{P}} \approx 26$ .

Using (9) in the approximation (8) violates unitarity. We can observe from this that inelasticity effects are important in the determination of the FSI phases [18]. As matter of fact, let us parametrize them as in Ref. [18] by one effective state, with no extra phases. Then the  $S$ -matrix should be written as follows (neglecting a small phase  $\varphi = -0.01$  in  $\sqrt{\mathcal{P}}$ ):

$$(B \rightarrow K^* \rho) \quad S \approx \begin{pmatrix} 0.64 & 0.77i \\ 0.77i & 0.64 \end{pmatrix} , \quad \sqrt{S} \approx \begin{pmatrix} 0.80 & 0.62(1+i) \\ 0.62(1+i) & 0.80 \end{pmatrix} ; \quad (16)$$

$$(B \rightarrow K^* \phi) \quad S \approx \begin{pmatrix} 0.77 & 0.64i \\ 0.64i & 0.77 \end{pmatrix} , \quad \sqrt{S} \approx \begin{pmatrix} 0.88 & 0.57(1+i) \\ 0.57(1+i) & 0.88 \end{pmatrix} ; \quad (17)$$

$$(B \rightarrow \rho \rho) \quad S \approx \begin{pmatrix} 0.58 & 0.82i \\ 0.82i & 0.58 \end{pmatrix} , \quad \sqrt{S} \approx \begin{pmatrix} 0.76 & 0.64(1+i) \\ 0.64(1+i) & 0.76 \end{pmatrix} . \quad (18)$$

This shows that even neglecting the effect of the non leading Regge trajectories, final state interactions due to inelastic effects parameterized by the Pomeron exchange can produce sizeable strong phases. This result agrees with the analogous findings of Refs. [19] and [18].

## B. Regge trajectories

Let us now consider the contribution of the charmed Regge trajectories. They are present in the  $B \rightarrow K^* \phi$  amplitude, in the  $I = 1/2$  amplitude for the decay  $B \rightarrow K^* \rho$  and in  $I = 0$  amplitude for  $B \rightarrow \rho^+ \rho^-$ . They do not contribute to the  $B^+ \rightarrow \rho^+ \rho^0$  decay channel because the final state has  $I = 2$  and the two charmed mesons can only have either  $I = 0$  or  $I = 1$ .

Including charmed Regge trajectories the  $S$  matrix can be written for the generic  $B \rightarrow VV$  case as follows

$$S = \mathcal{P} + \mathcal{D} + \mathcal{D}^* . \quad (19)$$

Here  $\mathcal{P}$  is the Pomeron contribution discussed above; we note that  $\mathcal{P}_{ij} = \mathcal{P}_i \delta_{ij}$ .  $\mathcal{D}$  and  $\mathcal{D}^*$  are reggeized amplitudes corresponding to the  $D$  and  $D^*$  Regge trajectories. For  $B \rightarrow K^* \phi$ ,  $K^* \rho$  decays they connect the state  $|K^* V\rangle$  to the other states  $|D_s D\rangle$ ,  $|D_s D^*\rangle$ ,  $|D_s^* D\rangle$ ,  $|D_s^* D^*\rangle$ . For  $B^0 \rightarrow \rho^+ \rho^-$  they connect the state  $|\rho^+ \rho^-\rangle$  to the states  $|D^+ D^-\rangle$ ,  $|D^{*+} D^-\rangle$ ,  $|D^+ D^{*-}\rangle$ ,  $|D^{*+} D^{*-}\rangle$ . Since all the Regge contributions are exponentially suppressed one can make the approximation

$$\sqrt{S} \approx \sqrt{\mathcal{P}} + \frac{1}{2} \mathcal{P}^{-1/2} (\mathcal{D} + \mathcal{D}^*) . \quad (20)$$

We discuss explicitly the case  $B \rightarrow K^* \phi$ , the treatment of the other cases being similar. Neglecting other inelastic effects we consider a  $5 \times 5$   $S_{ij}$  matrix, where  $i = 1, 2, 3, 4, 5$  represent respectively the states  $|D_s D\rangle$ ,  $|D_s D^*\rangle$ ,  $|D_s^* D\rangle$ ,

$|D_s^* D^*\rangle, |K^* \phi\rangle$ . The kinematic factors are as follows:  $\ell_j = s(s-4m_D^2), j=1, \dots, 4, \ell_5 = s^2, \rho_j = \sqrt{(s-4m_D^2)/s}, j=1, \dots, 4, \rho_5 = 1$ . We work in the approximation  $m_D^2 = m_{D_s}^2 = m_{D^*}^2 = m_{D_s^*}^2$  and  $m_{K^*} = m_\rho = m_\phi = m_V \sim 0.9$  GeV with  $s = m_B^2$ . The integration limits are for the elastic contribution:  $t_- = 0$  and  $t_+ = -s + 4m_V^2$ ; for the inelastic contributions:  $t_\mp = -s/2 + m_V^2 + m_D^2 \pm s/2\sqrt{1-4m_V^2/s}\sqrt{1-4m_D^2/s}$ . Therefore

$$A(B \rightarrow K^* \phi)_\lambda = \sqrt{\mathcal{P}} A_{b,\lambda}^{(5)} + \sum_{k=1}^4 \sum_{\lambda_i} \frac{1}{2} \mathcal{P}^{-1/2} (\mathcal{D} + \mathcal{D}^*)_{\lambda_i, \lambda}^{(k)} A_{b,\lambda_i}^{(k)}. \quad (21)$$

Let us consider the Regge amplitudes  $R = \mathcal{D}, \mathcal{D}^*$ :

$$R^{(k)}(s) = \frac{2i}{16\pi} \sqrt[4]{\frac{s-4m_D^2}{s}} \frac{1}{\sqrt{s(s-4m_D^2)}} \int_{t_+}^{t_-} dt R^{(k)}(s, t), \quad (22)$$

with  $t_\pm$  given above. We assume the general parametrization

$$R^{(k)}(s, t) = -\beta^R \frac{1 + (-)^{s_R} e^{-i\pi\alpha_R(t)}}{2} \Gamma(l_R - \alpha_R(t)) (\alpha')^{1-l_R} (\alpha')^{s_R} \quad (23)$$

as suggested in [27]. We notice the Regge poles at  $l_R - \alpha_R(t) = 0, -1, -2, \dots$ ; for  $R = \mathcal{D}$  we have  $s_R = \ell_R = 0$  and, for  $R = \mathcal{D}^*$ ,  $s_R = \ell_R = 1$ . Near  $t = m_R^2$ , (23) reduces to

$$R \approx \beta^R \frac{s^{s_R}}{(t - m_R^2)} \quad (24)$$

which allows to identify  $\beta^R$  as the product of two on-shell coupling constants. Let us write

$$\beta^R = \beta_{D_s^{(*)} K^*} \beta_{D^{(*)} V}. \quad (25)$$

Using the effective lagrangian approach [28] we can compute the residues by identifying them with the coupling constants for  $t \sim m_R^2$ . The numerical results are in Table V; they are obtained by the following values of the constants defined in [28]:  $g_V = 5.8$ ,  $\lambda = 0.56$  GeV $^{-1}$ ,  $\beta = 0.9$ , which represents an updated fit, see [16] for details.

Residue	$\mathcal{D}$	Num. values	$\mathcal{D}^*$	Num. values
$\beta_{DV}^0$	$\beta g_V m_V / \sqrt{2}$	+2.84	0	0
$\beta_{DV}^\pm$	$\beta g_V m_D$	+9.76	$\sqrt{2} \lambda g_V m_D$	+8.59
$\beta_{D^*V}^{0,0}$	0	0	$\frac{m_V g_V}{2 m_D} (\beta - 4\lambda m_D)$	-3.93
$\beta_{D^*V}^{\pm,\pm}$	$\sqrt{2} \lambda g_V m_D^2$	+16.1	$2 \lambda g_V m_D$	+12.1
$\beta_{D^*V}^{0,\pm}$	$2 \lambda g_V m_D^2$	+22.7	$\frac{g_V}{\sqrt{2}} (\beta - 2\lambda m_D)$	-4.90
$\beta_{D^*V}^{\pm,0}$	$2 \lambda g_V m_V m_D$	+9.35	0	0
$\beta_{D^*V}^{\pm,\mp}$	$\sqrt{2} \lambda g_V m_D^2$	+16.1	0	0

TABLE V: Regge residues  $\beta^{\lambda_i, \lambda}$  of the poles  $\mathcal{D}^*$  and  $\mathcal{D}$ ;  $\lambda_i$  is the polarization of the charmed meson,  $\lambda$  that of the light vector meson. The numerical results are obtained with  $g_V = 5.8$ ,  $\lambda = 0.56$  GeV $^{-1}$ ,  $\beta = 0.9$ , see [16].  $SU(3)_f$  nonet symmetry has been assumed for the evaluation of the residues.

It is important to stress that, differently from the Pomeron, which is mainly helicity conserving, Regge charmed trajectories have several helicity-flip residues. In particular they can change longitudinal into transverse polarizations, see e.g.  $\beta_{D^*V}^{0,\pm}$ . In the next section we will discuss these effects in the context of  $B \rightarrow VV$  decays.

Next step is the calculation of the trajectories  $\alpha_D(t)$  and  $\alpha_{D^*}(t)$ . To do this we use the model described in the Appendix. For charmed mesons such as  $D$  and  $D^*$  (we do not distinguish between  $D$  and  $D_s$ ) the Regge trajectories are not linear in the whole  $t$  range. Due to the exponential suppression of the high  $|t|$  range, only the small  $t$  region is of interest and here we can approximately write

$$\alpha_D = s_D + \alpha_0 + \alpha' t, \quad \alpha_{D^*} = s_{D^*} + \alpha_0 + \alpha' t, \quad (26)$$

with  $s_D = 0$ ,  $s_{D^*} = 1$ . From the results of the Appendix we have  $\alpha_0 = -1.8$ . As to the value of the slope  $\alpha'$ , linearizing the trajectory as in the dashed-dotted line of Fig. 4 (right side) one gets  $\alpha' = 0.33 \text{ GeV}^{-2}$ . This formula overestimates the mass of the  $D, D^*$  system by 15%. Fitting these masses would give the value  $\alpha' = 0.45 \text{ GeV}^{-2}$ ; from these results one can estimate a range 0.33-0.45  $\text{GeV}^{-2}$  for  $\alpha'$ . In a conservative vein we double this range to take into account other theoretical uncertainties (arising from the model adopted in the Appendix) and use therefore

$$\alpha_0 = -1.8, \quad \alpha' = (0.39 \pm 0.12) \text{ GeV}^{-2}. \quad (27)$$

#### IV. NUMERICAL RESULTS AND DISCUSSION

In the present approach one can identify two kinds of theoretical uncertainties, one related to the choice of the semileptonic  $B \rightarrow V$  form factors, the other to the parameters of the Regge amplitudes. To start with we fix the form factors, by choosing the numerical results obtained by the Light Cone sum rules approach [21]. The bare amplitudes can be found in Tables II and III; for the Regge parameters we use eq. (27), limiting the analysis to the central value and the two extremes of the  $\alpha'$  range. The numerical results are presented in Table VI.

Process	$\Gamma_L/\Gamma$	$\Gamma_\perp/\Gamma$	$\Gamma_\parallel/\Gamma$	B.R. $\times 10^6$
$B \rightarrow K^* \phi$	0.31	0.1	0.59	35
	0.73	0.06	0.20	15
	0.87	0.05	0.08	12
$B \rightarrow K^{*+} \rho^0$	0.26	0.12	0.61	19
	0.72	0.08	0.20	6.2
	0.89	0.06	0.05	4.9
$B \rightarrow K^{*0} \rho^+$	0.18	0.11	0.71	35
	0.61	0.07	0.32	9.9
	0.84	0.05	0.11	7.2
$B^+ \rightarrow \rho^+ \rho^0$	0.95	0.03	0.03	14
$B^0 \rightarrow \rho^+ \rho^-$	0.86	0.01	0.13	28
	0.93	0.02	0.05	26
	0.94	0.02	0.04	26

TABLE VI: Results for the various  $B$  decay channels obtained with the form factors as in [21]. For each decay channel the Regge slope of the charmed trajectories is, from top to bottom,  $\alpha' = (0.27, 0.39, 0.51) \text{ GeV}^{-2}$ . There is no Regge contribution to  $B^+ \rightarrow \rho^+ \rho^0$  so that the only FSI effect here is the elastic one. All the Branching Ratios are evaluated using  $\tau_B = 1.67 \text{ ps}$ .

We note that for  $B \rightarrow K^* V$  decays the smallest value of  $\alpha'$  corresponds to the largest contribution from the Regge trajectories. The Table VI shows that the main effect of the Regge poles for the channels with a  $K^*$  in the final state is the reduction of the longitudinal polarization fraction and the increase of the other fractions. This is due to the effect mentioned in subsection III B, i.e. the existence of helicity flip residues changing longitudinal into transverse polarizations. On the other hand the transverse polarization fraction  $\Gamma_\perp/\Gamma$  cannot increase beyond 10%-12%.

A more detailed numerical analysis for the channel  $B \rightarrow K^{*+} \rho^0$  can be found in Fig. 1 that shows the variation of the branching ratio and the polarization fractions versus the slope  $\alpha'$ . A detailed analysis of the  $K^* \phi$  channel will be presented below. Finally we observe that, as expected, the  $\rho\rho$  channels get negligible or vanishing contribution from the Regge poles. For the  $\rho^+ \rho^-$  channel this is due to the absence of the Cabibbo enhancement; for the  $\rho^+ \rho^0$  decay mode there is no Regge contribution because the final state is a pure  $I = 2$  state. If the explanation presented here is valid, the large fraction  $\Gamma_L/\Gamma$  for  $B \rightarrow \rho\rho$  (see Table I) is a consequence of the negligible role of the charmed Regge poles.

Let us comment on the discrepancies between the theoretical results of Table VI, Fig. 1 and experimental data. They might point to new physics, but a simpler possibility is an interplay between final state interactions and form factors. An example is offered by the channel  $K^* \phi$ . Here to get a small longitudinal polarization fraction one would prefer a small value of  $\alpha'$ . Small values of  $\alpha'$ , however, produce values for the branching ratio much higher than the data. As discussed in the Introduction, the dominance of  $\Gamma_L/\Gamma$  is a consequence of the chiral structure of the currents in the standard model and the  $m_b \rightarrow \infty$  limit. The only way to reduce it without invoking new physics is to show the existence of soft effects in the standard model. Our analysis shows that these effects can be generated by rescattering effects parametrized by the Regge model. On the other hand the high value of the branching ratio might be due to

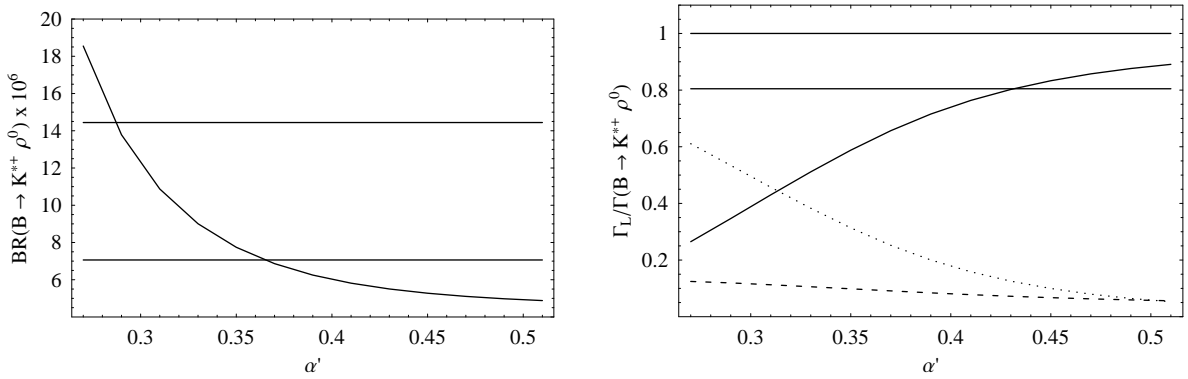


FIG. 1: Comparison between theoretical predictions based on the form factors of Ref. [21] and the experimental data for the channel  $B^+ \rightarrow K^{*+} \rho^0$ . On the left: The  $B.R. \times 10^6$  as a function of the parameter  $\alpha'$  giving the slope of the charmed Regge trajectories. Continuous straight lines give the experimental interval (see Table I). On the right: Continuous lines give the fraction  $\Gamma_L/\Gamma$ , the dashed line is the fraction  $\Gamma_\perp/\Gamma$  and the dotted line the fraction  $\Gamma_\parallel/\Gamma$ . Units of  $\alpha'$  are  $\text{GeV}^{-2}$ . We use  $\tau_B = 1.67$  ps.

the choice of the form factors of Ref. [21]. To deal with this problem we consider a different set of form factors. Since in  $B \rightarrow VV$  decays only small  $q^2$  are involved, the Lattice QCD determinations are unreliable because of the large extrapolations they would need. The best alternative to Light Cone sum rules are the traditional QCD sum rules. In [22] such a calculation is performed; we have reported these predictions in Table II. The authors in [22] only consider the  $b \rightarrow s$  transition, and therefore their results can be only applied to the channel  $B \rightarrow \phi K^*$  (in [29] also the transition  $b \rightarrow u$  was considered, but with a set of parameters different from [22], which renders the comparison difficult). In figures 2 and 3 we report the branching ratio and the fraction  $\Gamma_L/\Gamma$  as functions of the slope  $\alpha'$  of the charmed Regge trajectories for the parametrizations [22] and [21]. As to the other polarization fractions,  $\Gamma_\parallel/\Gamma$  and  $\Gamma_\perp/\Gamma$  for the form factors of Ref. [21] can be found in Table VI. The analogous figures for the form factors of [22] are  $\Gamma_\perp/\Gamma = (0.12, 0.12, 0.12)$  and  $\Gamma_\parallel/\Gamma = (0.74, 0.40, 0.20)$  for  $\alpha' = (0.27, 0.39, 0.51)$   $\text{GeV}^{-2}$ .

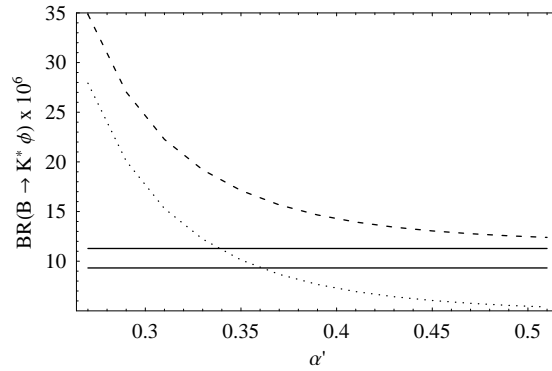


FIG. 2:  $BR(B \rightarrow K^* \phi) \times 10^6$  as a function of the parameter  $\alpha'$  giving the slope of the charmed Regge trajectories. Continuous straight lines give the experimental interval (see Table I). Dashed lines are theoretical predictions based on the form factors of ref.[21]; dotted lines are based on the form factors of ref. [22]. Units of  $\alpha'$  are  $\text{GeV}^{-2}$ .

Fig. 2 shows that much smaller values of the branching ratio are obtained by the QCD sum rules form factors of Ref. [22] (dotted lines) for  $\alpha'$  around its central value; Fig 3 shows that for the same values of  $\alpha'$  satisfactory results for  $\Gamma_L/\Gamma$  are obtained. Finally  $\Gamma_\perp/\Gamma$  gets a value smaller, but still compatible within  $2\sigma$ , with the BaBar result (4).

These results show that data on the polarization fractions for the  $B \rightarrow K^* \phi$  decay channel might be explained as the effect of two converging factors: an appropriate set of form factors [22] and the presence of final state interactions computed by the Regge approach. It remains to be seen however how QCD sum rules and Regge phenomenology would work for the other channels  $B \rightarrow K^* \rho$  and  $B \rightarrow \rho \rho$ , an issue we plan to deal with in the future.



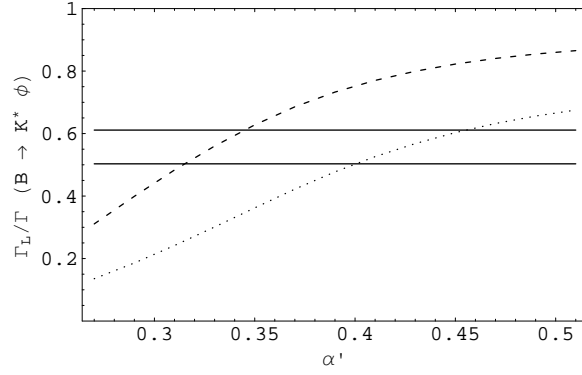


FIG. 3:  $\Gamma_L/\Gamma(B \rightarrow K^* \phi)$  as a function of the parameter  $\alpha'$  giving the slope of the charmed Regge trajectories. Continuous straight lines give the experimental interval (see Table I). Dashed lines are theoretical predictions based on the form factors of ref.[21]; dotted lines are based on the form factors of ref. [22]. Units of  $\alpha'$  are  $\text{GeV}^{-2}$ . We use  $\tau_B = 1.67$  ps.

## V. APPENDIX: A MODEL FOR REGGE TRAJECTORIES

For non charmed Regge poles,  $\alpha_R(t)$  is phenomenologically given by

$$\alpha_R(t) = s_R + \alpha'(t - m_R^2) \quad (28)$$

with the universal slope:  $\alpha' = 0.93 \text{ GeV}^{-2}$ . This behavior can be reproduced by a potential model, which gives the Regge formula the meaning of an exchange of infinitely many particles. To compute their spectrum one solves a Schroedinger equation and one shows that the slope is related to the string tension responsible of the confining part of the potential.

To be more specific we consider a bound state comprising a quark and an antiquark. For the bound state problem we consider the Salpeter equation (Schrödinger equation with relativistic kinematics):

$$\left( \sqrt{\mathbf{p}_1^2 + m_1^2} + \sqrt{\mathbf{p}_2^2 + m_2^2} + V(r) \right) \psi(\mathbf{r}) = E\psi(\mathbf{r}) \quad (29)$$

where  $m_j$  are quark masses,  $V(r)$  is the potential energy and  $r = |\mathbf{r}_1 - \mathbf{r}_2|$ . In the meson rest frame  $E$  is the meson mass  $M$  and  $\mathbf{p}_1^2 = \mathbf{p}_2^2 = -\hbar^2 \nabla^2$ . The bound state equation can be solved for arbitrarily large quantum numbers  $n$  and  $\ell$  (radial and orbital quantum numbers) by the WKB method [30]. We assume the potential

$$V(r) = V_0 + \mu^2 r \quad (30)$$

which is of course a simplification, but however able to show the linearity of Regge trajectories;  $\mu$  is the string tension and  $V_0$  is a constant negative term mimicking a repulsive core.

The WKB formula for this potential gives the result [30] (in units of string tension)

$$\int_0^\sigma dr \sqrt{\frac{(M - V(r))^2}{4} - \frac{m_1^2 + m_2^2}{2} + \frac{(m_1^2 - m_2^2)^2}{4(M - V(r))^2}} = \pi \left( n + \frac{\ell}{2} + \frac{3}{4} \right) \quad (31)$$

where  $\sigma = M - V_0 - m_1 - m_2$ . For light quarks we take for the constituent quark masses the values  $m_1 = m_2 = 300$  MeV. In units of string tension we get, for  $V_0 = -1.923$  and  $n = 0$  the Chew-Frautschi plot of Fig. 4 (left side) showing the almost linear Regge trajectory. It is given by Eq. (28) with  $s_R = 0$  since no spin term has been added to the potential in (30). For  $\alpha = \ell$  we find successive squared meson masses. The Regge trajectory has slope  $\alpha' = 0.25/\mu^2$ . For  $\mu = 0.52 \text{ GeV}$  we get a phenomenologically acceptable value of  $\alpha' \sim 0.9 \text{ GeV}^{-2}$ . The mass of low-lying meson with  $\ell = 0$  made up by up/down quarks turns out to be  $\sim 800$  MeV, an acceptable value as well.

We can now repeat the exercise for the  $D, D^*$  mesons. We use again  $m_1 = 300$  MeV and put for the charm quark  $m_2 = m_c = 1.7 \text{ GeV}$ . The result is reported on the right in Fig. 4. One can observe some deviations from linearity. The minimum value is given by kinematics as  $t = 4$  in units of the string tension. Solid line gives the WKB solution of the bound state equation; for small values we can still approximate  $\alpha(t)$  by a straight line (dashed-dotted line in

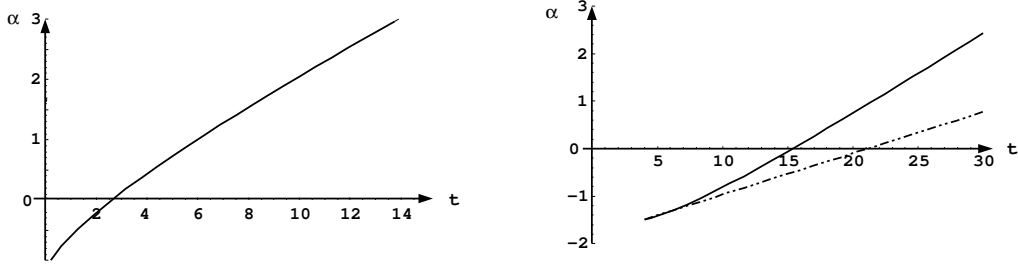


FIG. 4: On the left: Chew-Frautschi plot for a  $q\bar{q}$  meson of mass  $M$  made up by light quarks with masses of 0.577 in units of string tension ( $\sim 300$  MeV). On the horizontal axes  $t = M^2$  in units of string tension, on the vertical axis the Regge trajectory  $\alpha(t)$  approximately given by  $\alpha(t) = s_R + \alpha'(t - m_R^2)$  with  $s_R = 0$ , see text. The meson masses correspond to successive values of  $\alpha = \ell = 0, 1, \dots$ . On the right: Chew-Frautschi plot for a  $q\bar{Q}$  meson of mass  $M$  made up by a charm quark and a light quark ( $m_c = 1.7$  GeV,  $m_q = 0.3$  GeV). On the horizontal axes  $t = M^2$  in units of string tension, on the vertical axis the Regge trajectory. Solid line gives the WKB solution of the bound state equation; dashed-dotted line a linear approximation in the small  $t$  region.

the figure), with  $\alpha(t) = \alpha_0 + \alpha't$  and  $\alpha_0 = -1.8$ ,  $\alpha' = 0.09/\mu^2 = 0.33 \text{ GeV}^{-2}$ .

- 
- [1] B. Aubert et al. (BABAR), Phys. Rev. Lett. **91**, 171802 (2003), hep-ex/0307026.
  - [2] B. Aubert et al. (BABAR), Phys. Rev. **D69**, 031102 (2004), hep-ex/0311017.
  - [3] K. F. Chen et al. (Belle), Phys. Rev. Lett. **91**, 201801 (2003), hep-ex/0307014.
  - [4] J. Zhang et al. (Belle), Phys. Rev. Lett. **91**, 221801 (2003), hep-ex/0306007.
  - [5] A. L. Kagan (2004), hep-ph/0405134.
  - [6] Y. Grossman, Int. J. Mod. Phys. **A19**, 907 (2004), hep-ph/0310229.
  - [7] P. Colangelo, F. De Fazio, and T. N. Pham, Phys. Lett. **B597**, 291 (2004), hep-ph/0406162.
  - [8] A. L. Kagan (2004), hep-ph/0407076.
  - [9] M. Bauer, B. Stech, and M. Wirbel, Z. Phys. **C34**, 103 (1987).
  - [10] J. Charles, A. Le Yaouanc, L. Oliver, O. Pene, and J. C. Raynal, Phys. Rev. **D60**, 014001 (1999), hep-ph/9812358.
  - [11] A. Gritsan (BABAR) (2004), <http://costard.lbl.gov/gritsan/RPM/BABAR-COLL-0028.pdf>.
  - [12] P. Colangelo, G. Nardulli, N. Paver, and Riazuddin, Z. Phys. **C45**, 575 (1990).
  - [13] M. Ciuchini, E. Franco, G. Martinelli, and L. Silvestrini, Nucl. Phys. **B501**, 271 (1997), hep-ph/9703353.
  - [14] C. Isola, M. Ladisa, G. Nardulli, T. N. Pham, and P. Santorelli, Phys. Rev. **D64**, 014029 (2001), hep-ph/0101118.
  - [15] C. Isola, M. Ladisa, G. Nardulli, T. N. Pham, and P. Santorelli, Phys. Rev. **D65**, 094005 (2002), hep-ph/0110411.
  - [16] C. Isola, M. Ladisa, G. Nardulli, and P. Santorelli, Phys. Rev. **D68**, 114001 (2003), hep-ph/0307367.
  - [17] R. Casalbuoni et al., Phys. Rept. **281**, 145 (1997), hep-ph/9605342.
  - [18] J. F. Donoghue, E. Golowich, A. A. Petrov, and J. M. Soares, Phys. Rev. Lett. **77**, 2178 (1996), hep-ph/9604283.
  - [19] G. Nardulli and T. N. Pham, Phys. Lett. **B391**, 165 (1997), hep-ph/9610525.
  - [20] K. M. Watson, Phys. Rev. **88**, 1163 (1952).
  - [21] P. Ball, ECONF **C0304052**, WG101 (2003), hep-ph/0306251.
  - [22] P. Colangelo, F. De Fazio, P. Santorelli, and E. Scrimieri, Phys. Rev. **D53**, 3672 (1996), hep-ph/9510403.
  - [23] A. Ali, G. Kramer, and C.-D. Lu, Phys. Rev. **D58**, 094009 (1998), hep-ph/9804363.
  - [24] S. Eidelman et al. (Particle Data Group), Phys. Lett. **B592**, 1 (2004).
  - [25] A. Donnachie and P. V. Landshoff, Phys. Lett. **B296**, 227 (1992), hep-ph/9209205.
  - [26] H.-q. Zheng, Phys. Lett. **B356**, 107 (1995), hep-ph/9504360.
  - [27] A. C. Irving and R. P. Worden, Phys. Rept. **34**, 117 (1977).
  - [28] R. Casalbuoni et al., Phys. Rept. **281**, 145 (1997), hep-ph/9605342.
  - [29] P. Ball and V. M. Braun, Phys. Rev. **D55**, 5561 (1997), hep-ph/9701238.
  - [30] P. Cea, P. Colangelo, G. Nardulli, G. Paiano, and G. Preparata, Phys. Rev. **D26**, 1157 (1982).